



# CHEMISTRY

## A European Journal



### Accepted Article

**Title:** Gold-Catalyzed Facile Synthesis and Crystal Structures of Benzene-/Naphthalene-based Bispentalenes as Organic Semiconductors

**Authors:** Kohei Sekine, Jürgen Schulmeister, Fabian Paulus, Katelyn P. Goetz, Frank Rominger, Matthias Rudolph, Jana Zaumseil, and A. Stephen K. Hashmi

This manuscript has been accepted after peer review and appears as an Accepted Article online prior to editing, proofing, and formal publication of the final Version of Record (VoR). This work is currently citable by using the Digital Object Identifier (DOI) given below. The VoR will be published online in Early View as soon as possible and may be different to this Accepted Article as a result of editing. Readers should obtain the VoR from the journal website shown below when it is published to ensure accuracy of information. The authors are responsible for the content of this Accepted Article.

**To be cited as:** *Chem. Eur. J.* 10.1002/chem.201805637

**Link to VoR:** <http://dx.doi.org/10.1002/chem.201805637>

Supported by  
**ACES**

WILEY-VCH

## COMMUNICATION

# Gold-Catalyzed Facile Synthesis and Crystal Structures of Benzene-/Naphthalene-based Bispentalenes as Organic Semiconductors

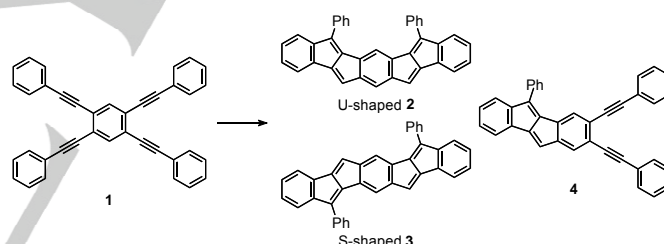
Kohei Sekine,<sup>[a]</sup> Jürgen Schulmeister,<sup>[a]</sup> Fabian Paulus,<sup>[b]</sup> Katelyn P. Goetz,<sup>[b]</sup> Frank Rominger,<sup>[a]</sup> Matthias Rudolph,<sup>[a]</sup> Jana Zaumseil,<sup>\*[b]</sup> and A. Stephen K. Hashmi<sup>\*[a,c]</sup>

**Abstract:** We describe the gold-catalyzed facile synthesis of U-shaped and S-shaped bispentalenes from easily available tetra(arylethynyl)-benzenes and -naphthalenes. The optoelectronic and transistor properties were also investigated. The selectivity between the U-shaped and S-shaped bispentalene isomers can be tuned by the bulkiness of the ligand and the substrates. The S-shaped naphthalene-based bispentalene shows a one dimensional face-to-face packing pattern in solid state and a good hole mobility, indicating that the S-shaped bispentalene core is highly suitable for transistor applications. The gold-catalyzed annulation of tetrynes provides a useful protocol in the synthesis of bispentalenes for organic semiconductors.

Homogeneous gold catalysis has received much attention in the last two decades.<sup>[1]</sup> Due to the mild carbophilic  $\pi$  Lewis acidity of the gold catalyst, nucleophilic addition reactions to unsaturated carbon-carbon multiple bonds were intensely developed. Side-by-side gold catalysts promote the annulation of diyne compounds, not only showing unique reaction patterns, but also contributing to the syntheses of complicated and/or highly  $\pi$ -conjugated compounds.<sup>[2]</sup>

The pentalene scaffold is of high interest for materials science due to its antiaromaticity<sup>[3]</sup> as much as structurally similar indenofluorene.<sup>[4]</sup> Due to the low stability of the pure pentalene core,<sup>[5]</sup> the synthesis and properties of monobenzopentalene and dibenzo[a,e]pentalene, which are stabilized by the flanking aromatic moieties, are well studied.<sup>[6]</sup> Due to the promising properties of  $\pi$ -extended pentalenes they are attractive as organic semiconductors. Dinaphtho[a,e]pentalene, dianthraceno[a,e]pentalene and the pyrrole-fused dibenzo[a,e]pentalene exhibit high hole mobilities,<sup>[7]</sup> while the thiophene-substituted dibenzo[a,e]pentalenes and diacenopentalene dicarboximides exhibit lower-lying LUMO levels suitable for n-type semiconductors.<sup>[6s, 8]</sup> Despite the development of  $\pi$ -extended pentalenes, the synthesis of bispentalenes is not yet well studied.<sup>[8]</sup> The achievement of palladium-catalyzed synthesis of bis(dibenzo)pentalenes from an internal alkyne and bromostyrene requires a multi-step

synthesis.<sup>[9b]</sup> Obviously, one of the most step-economic strategies for the synthesis of bis(dibenzo)pentalene is the annulation of 1,2,4,5-tetrakis(arylethynyl) benzene **1**, which potentially produces the U-shaped and S-shaped bis(dibenzo)pentalenes **2** and **3** as the second cyclization can occur onto both alkynes of the intermediate mono(dibenzo)pentalene **4** (Scheme 1). In the reported platinum-promoted annulation of tetrayne **1**, bispentalenes **2** and **3** were produced in poor selectivity and in low yields.<sup>[9a]</sup> In this context, a facile synthetic method is desirable for the supply and property evaluation of U-shaped and S-shaped bispentalene derivatives. Recently, we reported the (IPr)Au(NCMe)SbF<sub>6</sub>-catalyzed annulation of 1,2-di(arylethynyl)benzene produced dibenzo[a,e]pentalene derivatives *via* a vinyl cation species as a key intermediate.<sup>[6o]</sup> Herein, we present the gold-catalyzed annulation of tetrakis(arylethynyl)-benzenes and -naphthalenes for the synthesis of U-shaped and S-shaped bispentalene derivatives **2** and **3**. The opto-electronic and transistor properties of the obtained bispentalene derivatives are also reported.



**Scheme 1.** The synthetic strategy towards bispentalenes **2** and **3**.

First, various gold catalysts were examined with 1,2,4,5-tetrakis((4-pentylphenyl)ethynyl)benzene **1a** (Table 1). In the presence of (IPr)AuCl/AgNTf<sub>2</sub>, **1a** was completely consumed within 30 mins to afford the U-shaped **2a** in high selectivity (>20:1) in 82% yield (Entry 1). This result matches the previous work<sup>[6g]</sup>, where the selectivity for the U-shaped **2** was explained by the steric hindrance of the bulky IPr ligand and the peripheral aryl group at the second cyclization of the intermediate **4**. Based on these results, we hypothesized that if a less bulky ligand was employed, an S-shaped bis(dibenzo)pentalene **3a** might be feasible. As expected, a smaller carbene ligand (IMes)AuCl/AgNTf<sub>2</sub> (IMes; %Vbur = 36.5, IPr; %Vbur = 45.4)<sup>[10]</sup> afforded the mixture of U-shaped **2a** and S-shaped **3a** in ratios of 82:18 in 84% combined yield (Entry 2). The isomers were separable by silica gel column chromatography and the structures of **2a** and **3a** were unambiguously confirmed by X-ray crystal structure analysis.<sup>[11]</sup> **3a** shows a one dimensional  $\pi$ - $\pi$  stacking. The acyclic carbene gold catalyst L<sub>1</sub>AuCl (%Vbur = 36.9) afforded a 63% yield of a mixture of 64:36 **2a** to **3a** (Entry 3).

[a] Dr. K. Sekine, B. Mc. J. Schulmeister, Dr. F. Rominger, Dr. M. Rudolph and Prof. Dr. A. S. K. Hashmi  
Organisch-Chemisches Institut, Heidelberg University  
Im Neuenheimer Feld 270, 69120 Heidelberg, Germany  
E-mail: hashmi@hashmi.de

[b] Dr. F. Paulus, Dr. K. P. Goetz and Prof. Dr. J. Zaumseil  
Institute for Physical Chemistry, Universität Heidelberg  
Im Neuenheimer Feld 253, 69120 Heidelberg, Germany  
E-mail: zaumseil@uni-heidelberg.de

[c] Prof. Dr. A. S. K. Hashmi  
Chemistry Department, Faculty of Science  
King Abdulaziz University, Jeddah 21589, Saudi Arabia

Supporting information for this article is given via a link at the end of the document.

## COMMUNICATION

Smaller %Vbur carbene ligands, **L**<sub>2</sub>AuCl (%Vbur = 27.4, Entry 4) and (IDM)AuCl (%Vbur = 26.3, Entry 5) showed a ratio of 66:34 and 55:45, respectively, though **1a** remained and a relatively complex reaction mixture was produced. These results indicate that the selectivity for the U-shaped **2a** is dependent on the %Vbur of the applied ligands. SPhos (Entry 6), phosphite ligand **L**<sub>3</sub> (Entry 7) and triphenylphosphine ligand (Entry 8) gave the isomers **2a** and **3a** in ratios of 75:25, 66:34 and 50:50, respectively. The same dependency of the selectivity as the carbene ligands was also observed for the phosphorus ligands (Entries 6-8), underlining that the ligand size is crucial for the selectivity.

afforded **2b** and **3b** in a ratio of 57:43 in high combined yields (Entry 4). Fluoro-substituted tetrayne (**1c**) was converted by both IPr and **L**<sub>1</sub> ligands to **2c** and **3c** in high yields in a ratio of 92:8 (Entry 5) and 60:40 (Entry 6). The isomers of **2b** and **3b**, **2c** and **3c** were separable by silica gel column chromatography. The methyl-, H-, and 4-pentylphenyl-substitutions on outer aromatic moieties substrates **1d-1f** were selectively transformed with (IPr)AuCl to the corresponding U-shaped derivatives **2d-2f** in 92%, 67% and 53 yields (Entries 7, 9, and 11). With the smaller catalyst, the pentalenes **2d** and **3d** (73:27), **2e** and **3e** (69:31), and **2f** and **3f** (62:38) were produced in moderate-to-high combined yields (Entries 8, 10, and 12). Unfortunately, in the case of the substrates **1d-f**, the two isomers **2** and **3** are inseparable due to their poor solubility.

**Table 1.** Examination of different gold catalysts.

Entry <sup>[a]</sup>	Catalyst	%V <sub>Bur</sub>	Time	Yield ( <b>2a</b> + <b>3a</b> ) %	<b>2a</b> : <b>3a</b> <sup>[b]</sup>
1	(IPr)AuCl	45.4	30 min	82 <sup>[c]</sup>	>20:1
2	(IMes)AuCl	36.5	30 min	84	82:18
3	<b>L</b> <sub>1</sub> AuCl	36.9	30 min	63	64:36
4	<b>L</b> <sub>2</sub> AuCl	27.5	24 h	- <sup>[d]</sup>	66:34
5	(IDM)AuCl	26.3	24 h	- <sup>[d]</sup>	55:45
6	SPhosAuCl	53.7	20 h	39	75:25
7	<b>L</b> <sub>3</sub> AuCl	37.8	20 h	37	66:34
8	Ph <sub>3</sub> PAuCl	34.8	20 h	29	50:50

[a] **1a** (0.05 mmol), catalysts (0.005 mmol) in solvent (1.5 mL). [b] Ratios of **2a**:**3a** determined by <sup>1</sup>H NMR. [c] Isolated yield of **2a**. [d] Not full conversion.

Several substituents were examined next to synthesize the U-shaped and S-shaped **2** and **3** with (IPr)AuCl or **L**<sub>1</sub>AuCl in dichloromethane due to the improved solubility (Table 2). In the case of a methyl group on the aromatic core (**1b**), the reaction with (IPr)AuCl/AgNTf<sub>2</sub> was completed within 4 h to give **2b** and **3b** in 98% combined yield in a ratio of 77:23 (Entry 3). Compared to tetrayne **1a**, the reaction took longer and the ratio of S-shaped product **3b** increased. The smaller catalysts **L**<sub>1</sub>AuCl/AgNTf<sub>2</sub>

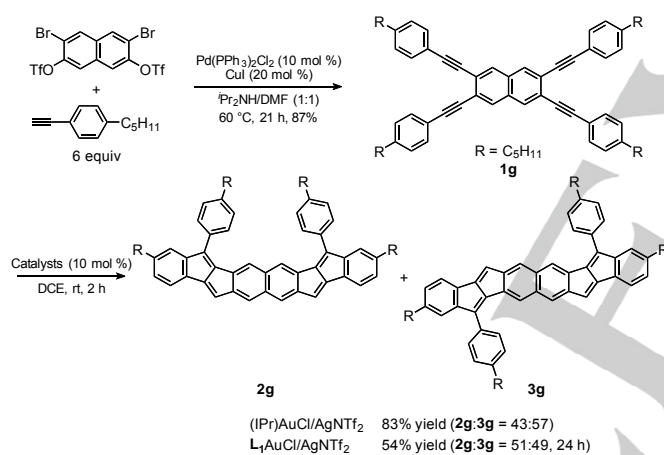
**Table 2.** Gold-catalyzed synthesis of bis(dibenzo)pentalene derivatives

Entry <sup>[a]</sup>	R <sup>1</sup>	R <sup>2</sup>	Catalyst	Time	Yield <b>2</b> /% <sup>[b]</sup> ( <b>2</b> : <b>3</b> )
1	C <sub>6</sub> H <sub>11</sub>	H	<b>1a</b> (IPr)AuCl	30 min	82
2	C <sub>6</sub> H <sub>11</sub>	H	<b>1a</b> <b>L</b> <sub>1</sub> AuCl	30 min	63 <sup>[c]</sup>
3	C <sub>6</sub> H <sub>11</sub>	Me	<b>1b</b> (IPr)AuCl	4 h	98 <sup>[c]</sup> (64:36) <sup>[d]</sup>
4	C <sub>6</sub> H <sub>11</sub>	Me	<b>1b</b> <b>L</b> <sub>1</sub> AuCl	4 h	90 <sup>[c]</sup> (77:23) <sup>[d]</sup>
5	C <sub>6</sub> H <sub>11</sub>	F	<b>1c</b> (IPr)AuCl	4 h	93 <sup>[c]</sup> (57:43) <sup>[d]</sup>
6	C <sub>6</sub> H <sub>11</sub>	F	<b>1c</b> <b>L</b> <sub>1</sub> AuCl	4 h	95 <sup>[c]</sup> (92:8) <sup>[d]</sup>
7	Me	H	<b>1d</b> (IPr)AuCl	1 h	92
8	Me	H	<b>1d</b> <b>L</b> <sub>1</sub> AuCl	18 h	94 <sup>[c]</sup> (73:27) <sup>[d]</sup>
9	H	H	<b>1e</b> (IPr)AuCl	1 h	67
10	H	H	<b>1e</b> <b>L</b> <sub>1</sub> AuCl	18 h	79 <sup>[c]</sup> (69:31) <sup>[d]</sup>
11	4-pentyl-C <sub>6</sub> H <sub>5</sub>	H	<b>1f</b> (IPr)AuCl	1 h	53
12	4-pentyl-C <sub>6</sub> H <sub>5</sub>	H	<b>1f</b> <b>L</b> <sub>1</sub> AuCl	18 h	58 <sup>[c]</sup> (62:38) <sup>[d]</sup>

## COMMUNICATION

[a] **1** (0.05 mmol), catalysts (0.005 mmol) in solvent (1.5 mL). [b] Isolated yield. [c] Yield of **2** and **3**. [d] Ratio of **2** and **3** determined by <sup>1</sup>H NMR.

Next, the gold catalytic system was applied to 2,3,6,7- and 1,2,5,6-tetra(arylethynyl)naphthalene **1g** and **1h** (Scheme 2 and 3). The reaction of **1g** with (IPr)AuCl/AgNTf<sub>2</sub> produced the bispentalenes **2g** and **3g** in 83% yield in a ratio of 43:57 (Scheme 2). It was assumed that the poorer selectivity of **2g** and **3g** was caused by the less steric repulsion of the peripheral phenyl groups and the gold catalyst during the second annulation step. This assumption can be underlined by a less pronounced effect for smaller carbene ligand **L1** (**2g**:**3g** = 51:49). The crystal packing of **3g** is shown in Figure 2. [11] The molecules construct a one dimensional columnar structure (Figure 2a; viewed in the b-c plane). Effective offset stackings between the plane cores of the bispentalene core and a T-shaped stacking between the peripheral phenyl rings are observed (Figure 2b and 2c). Tetrayne (**1h**) was also converted with (IPr)AuCl/AgNTf<sub>2</sub> and selectively afforded the corresponding bispentalene **5h** in 73% yield (Scheme 3). [11] The gold catalyst preferentially activated the less sterically hindered alkyne at the 2- and 6-position of **5h** due to the steric repulsion around the peri-position.



**Scheme 2.** Synthesis of **2g** and **3g** from 2,3,6,7-tetrakis(arylethynyl)naphthalene.

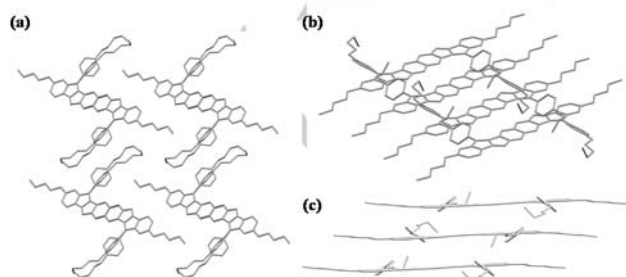
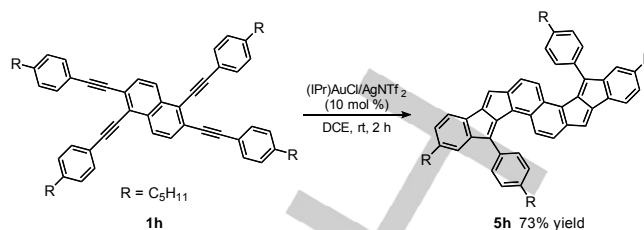


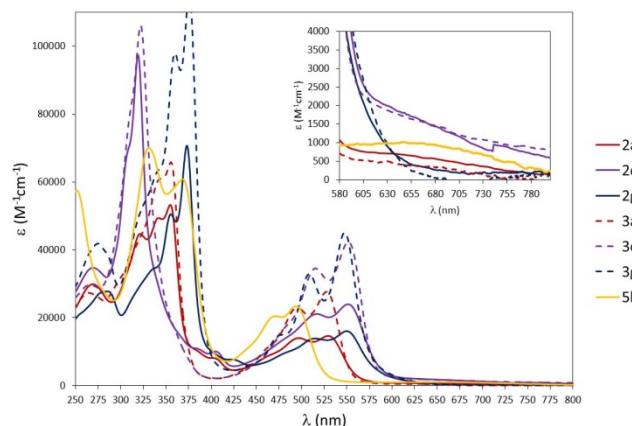
**Figure 2.** Packing diagrams of **3g** (hydrogen atoms are omitted for clarity)



**Scheme 3.** Synthesis of **5h**.

The optical properties of bispentalenes **2a**, **2c**, **2g**, **3a**, **3c**, **3g** and **5h** were examined by UV/Vis absorption spectroscopy (Figure 3). TD-DFT calculations at B3LYP-d3, cc-pVTZ level of theory (Supporting Information) suggest that the weak, broad, long wavelength absorption ( $\lambda_{\text{opt}}$  = 600–700 nm), which are slightly observed in the case of **2a**, **2c**, **3a**, **3c** and **5h**, can be attributed to the symmetry-forbidden HOMO-LUMO transitions. Based on the TD-DFT calculations, the absorptions of the second and third longest wavelength around 500 nm and 530 nm for **2a** can be assigned to the symmetry-allowed HOMO  $\rightarrow$  LUMO+1 and HOMO-1  $\rightarrow$  LUMO transitions (Table S3). In the case of **2g** and **3g** only the absorptions at lower wavelengths (**2g**;  $\lambda_{\text{opt}}$  = 550 and 516 nm, **3g**;  $\lambda_{\text{opt}}$  = 548 and 509 nm) are observed and the broad absorption for the HOMO-LUMO transitions ( $\lambda_{\text{opt}}$  = 600–700 nm) is not detected. TD-DFT calculations suggested the corresponding absorptions ( $\lambda_{\text{opt}}$  = 550 and 516 nm) of **2g** are derived from the symmetry-forbidden HOMO-1  $\rightarrow$  LUMO transitions ( $\lambda_{\text{cal}}$  = 514 nm) and the symmetry-allowed HOMO  $\rightarrow$  LUMO transitions ( $\lambda_{\text{cal}}$  = 487 nm). [12]

The HOMO and LUMO levels in CH<sub>2</sub>Cl<sub>2</sub> solution were estimated by cyclic voltammetry (Table S2). Compared to the corresponding dibenzopentalene **6** (LUMO = -3.05 eV,  $E_{\text{gap}}$  = 2.74 eV, Table S2) [6], the LUMO levels of **2a** (LUMO = -3.23 eV,  $E_{\text{gap}}$  = 1.98 eV) and **3a** (LUMO = -3.23 eV,  $E_{\text{gap}}$  = 1.99 eV) are lower by ~0.2 eV and the HOMO-LUMO energy gap are considerably smaller, indicating a significant effect of the  $\pi$ -extended system onto the LUMO level and the HOMO-LUMO gap. The fusing pattern of the naphthalene-based bispentalenes **2g**, **3g** and **5h** dramatically changes the HOMO-LUMO gaps. The gap of **2g** ( $E_{\text{gap}}$  = 2.25 eV) and **3g** ( $E_{\text{gap}}$  = 2.28 eV) is larger than that of **5h** ( $E_{\text{gap}}$  = 1.95 eV). [12]



## COMMUNICATION

**Figure 3.** UV absorption of **2a**, **2c**, **2g**, **3a**, **3c**, **3g** and **5h**.

The solid-state  $\pi$ -stacking of the S-shaped bispentalenes **3a** and **3g** indicates that they could display semiconducting behavior, inspiring us to fabricate field-effect transistors (FETs). The zone-casting method is suitable for film fabrication due to the one-dimensional nature of the crystal structures, as this method is known to yield arrays of aligned crystalline ribbons under proper processing conditions.<sup>[13]</sup> For the molecule **3g**, a slow casting speed of  $0.2 \text{ mm}\cdot\text{s}^{-1}$  on substrates of silicon/silicon dioxide/benzocyclobutene (BCB) results in “feathered” ribbons aligned at the micro scale, as seen in both optical and atomic force microscopy (AFM) images (Fig. 4a, 4b). The application of similar casting conditions to **3a** results in films with an amorphous appearance. The evaporation of gold source/drain electrodes to form a bottom gate, top contact FET geometry (inset of Fig. 4c) allows for hole injection and accumulation in **3g**. Representative transfer and output characteristics are shown in Fig. 4c, d, and average device parameters based on 75 devices with different channel lengths are shown in Table 3. The hole mobility ( $\mu$ ), determined for the saturation regime using the gradual channel approximation, exhibits moderate gate voltage ( $V_{GS}$ ) dependence, ranging from approximately  $0.1 \text{ cm}^2\text{V}^{-1}\text{s}^{-1}$  at the turn-on point to a minimum of  $0.07 \text{ cm}^2\text{V}^{-1}\text{s}^{-1}$  at the end of the measurement range. The maximum mobility achieved was  $0.25 \text{ cm}^2\text{V}^{-1}\text{s}^{-1}$ . The origin of the gate-source voltage dependence is unknown and currently under investigation. Nonetheless, these results suggest that the core of the molecule is highly suitable for transistor applications, and may show more ideal performance and higher charge-carrier mobility upon exchange of the solubilizing groups.

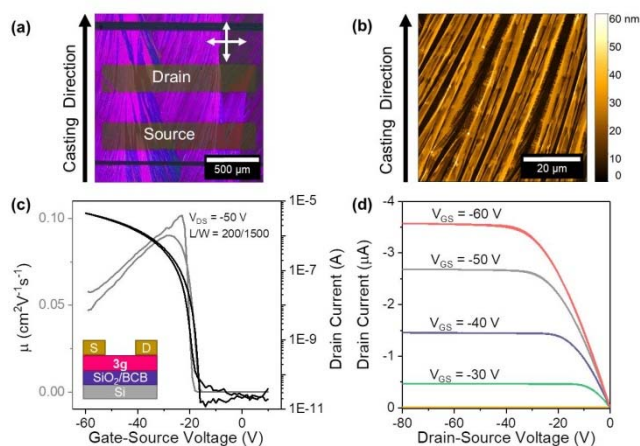


**Figure 4.** Field-effect transistors of **3g** fabricated using the zone-casting method. a) An optical image of the film under cross-polarized light, and b) a  $60 \mu\text{m} \times 60 \mu\text{m}$  AFM image of the aligned ribbon arrays. The fast scan direction of the AFM image is roughly perpendicular to the casting direction. c) The transfer characteristics and the gate-source voltage dependence of the charge-carrier mobility for a source-drain voltage ( $V_{DS}$ ) of  $-50 \text{ V}$ , with an inset depicting the FET schematic (S/D are the source/drain electrodes). d) The output characteristics of the FET.

**Table 3.** Transport properties of TFTs with **3g**.

Peak mobility (saturation) ( $\text{cm}^2\text{V}^{-1}\text{s}^{-1}$ )	Mobility at $V_{GS} = -60 \text{ V}$ ( $\text{cm}^2\text{V}^{-1}\text{s}^{-1}$ )	Threshold voltage (V)	$I_{on}/I_{off}$
$0.13 \pm 0.05$	$0.07 \pm 0.03$	$-20 \pm 4$	$10^5$

In conclusion, we developed a convenient synthetic method for U-shaped and S-shaped bispentalenes from readily available tetra(arylethynyl)-benzenes/-naphthalenes. Carbene ligands are suitable for the annulation reaction and the bulkiness of the ligand has a significant effect on the ration between the two U-shaped and S-shaped isomers. The S-shaped **3a** and **3g** showed a one-dimensional face-to-face packing pattern. The  $\pi$ -extended bispentalene is effective for the shrink of the HOMO-LUMO energy gap. Evaluation of the transistor property revealed that S-shaped **3g** shows a reasonable hole mobility ( $0.1 \text{ cm}^2\text{V}^{-1}\text{s}^{-1}$ ) and the bispentalene core is highly suitable for transistor applications. Further applications based on the bispentalene structure are under investigation.

## Acknowledgements

The authors are grateful to funding by the DFG (SFB 1249-NHeteropolyzyklen als Funktionsmaterialien). We thank Michael Töpfer of Fraunhofer IZM, Berlin, Germany, for generously providing us with the BCB Cycloctene polymer.

**Keywords:** gold catalysis • pentalene • polycyclic aromatic hydrocarbons • tetrayne • organic-field-effect transistor

- (a) D. Pflästerer, A. S. K. Hashmi, *Chem. Soc. Rev.* **2016**, *45*, 1331; (b) R. Dorel, A. M. Echavarren, *Chem. Rev.* **2015**, *115*, 9028; (c) L. Zhang, *Acc. Chem. Res.* **2014**, *47*, 877; (d) L. P. Liu, G. B. Hammond, *Chem. Soc. Rev.* **2012**, *41*, 3129; (e) H. Ohno, *Isr. J. Chem.* **2013**, *53*, 869; (f) A. Fürstner, *Chem. Soc. Rev.* **2009**, *38*, 3208; (g) N. Bongers, N. Krause, *Angew. Chem. Int. Ed.* **2008**, *47*, 2178; (h) A. Fürstner, P. W. Davies, *Angew. Chem. Int. Ed.* **2007**, *46*, 3410; (i) A. S. K. Hashmi, G. J. Hutchings, *Angew. Chem. Int. Ed.* **2006**, *45*, 7896; (j) A. S. K. Hashmi, *Chem. Rev.* **2007**, *107*, 3180; (k) D. J. Gorin, F. D. Toste, *Nature* **2007**, *446*, 395; (l) for early results, see: A. S. K. Hashmi, L. Schwarz, J.-H. Choi, T. M. Frost, *Angew. Chem. Int. Ed. Engl.* **2000**, *39*, 2285.
- A. M. Asiri, A. S. K. Hashmi, *Chem. Soc. Rev.* **2016**, *45*, 4471.
- H. Hopf, *Angew. Chem. Int. Ed.* **2013**, *52*, 12224.
- Overview of indenofluorenes (a) C. K. Frederickson, B. D. Rose, M. M. Haley, *Acc. Chem. Res.* **2017**, *50*, 977. As organic semiconductors (b) D. T. Chase, A. G. Fix, S. J. Kang, B. D. Rose, C. D. Weber, Y. Zhong, L. N. Zakharov, M. C. Lonergan, C. Nuckolls, M. M. Haley, *J. Am. Chem. Soc.* **2012**, *134*, 10349; (c) J. L. Marshall, K. Uchida, C. K. Frederickson, C. Schütt, A. M. Zeidell, K. P. Goetz, T. W. Finn, K. Jarolimek, L. N. Zakharov, C. Risko, R. Herges, O. D. Jurchescu, M. M. Haley, *Chem. Sci.* **2016**, *7*, 5547; (d) J.-D. Peltier, B. Heinrich, B. Donnio, J. Rault-Berthelot, E. Jacques, C. Poriel, *ACS Appl. Mater. Interfaces* **2017**, *9*, 8219.
- T. Bally, S. Chai, M. Neuenschwander, Z. Zhu, *J. Am. Chem. Soc.* **1997**, *119*, 1869.
- Review for the synthesis and optoelectronic properties of pentalenes, please see (a) M. Saito, *Symmetry* **2010**, *2*, 950. For recent publications

## COMMUNICATION

- about monobenzopentalene, see (b) P. Rivera-Fuentes, M. von Wantoch Rekowski, W. B. Schweizer, J.-P. Gisselbrecht, C. Boudon, F. Diederich, *Org. Lett.* **2012**, *14*, 4066; (c) G. London, M. von Wantoch Rekowski, O. Dumele, W. B. Schweizer, J.-P. Gisselbrecht, C. Boudon, F. Diederich, *Chem. Sci.* **2014**, *5*, 965; (d) S. Kato, S. Kuwako, N. Takahashi, T. Kijima, Y. Nakamura, *J. Org. Chem.* **2016**, *81*, 7700. For dibenzopentalene, see (e) K. Katsumoto, C. Kitamura, T. Kawase, *Eur. J. Org. Chem.* **2011**, 4885; (f) M. Saito, Y. Hashimoto, T. Tajima, K. Ishimura, S. Nagase, M. Minoura, *Chem. Asian J.* **2012**, *7*, 480; (g) A. S. K. Hashmi, M. Wieteck, I. Braun, P. Nosel, L. Jongbloed, M. Rudolph, F. Rominger, *Adv. Synth. Catal.* **2012**, *354*, 555; (h) C. Chen, M. Harhausen, R. Liedtke, K. Bussmann, A. Fukazawa, S. Yamaguchi, J. L. Petersen, C. G. Daniliuc, R. Fröhlich, G. Kehr, G. Erker, *Angew. Chem. Int. Ed.* **2013**, *52*, 5992; (i) T. Maekawa, Y. Segawa, K. Itami, *Chem. Sci.* **2013**, *4*, 2369; (j) J. Zhao, K. Oniwa, N. Asao, Y. Yamamoto, T. Jin, *J. Am. Chem. Soc.* **2013**, *135*, 10222; (k) J. Shen, D. Yuan, Y. Qiao, X. Shen, Z. Zhang, Y. Zhong, Y. Yi, X. Zhu, *Org. Lett.* **2014**, *16*, 4924; (l) C. Chen, M. Harhausen, A. Fukazawa, S. Yamaguchi, R. Fröhlich, C. G. Daniliuc, J. L. Petersen, G. Kehr, G. Erker, *Chem. Asian J.* **2014**, *9*, 1671; (m) G. London, M. von Wantoch Rekowski, O. Dumele, W. B. Schweizer, J.-P. Gisselbrecht, C. Boudon, F. Diederich, *Chem. Sci.* **2014**, *5*, 965; (n) B. Wei, H. Li, W.-X. Zhang, Z. Xi, *Organometallics* **2016**, *35*, 1458. (o) T. Wurm, J. Bucher, S. B. Duckworth, M. Rudolph, F. Rominger, A. S. K. Hashmi, *Angew. Chem. Int. Ed.* **2017**, *56*, 3364; (p) K. Takahashi, S. Ito, R. Shintani, K. Nozaki, *Chem. Sci.* **2017**, *8*, 101; (q) H. Oshima, A. Fukazawa, S. Yamaguchi, *Angew. Chem. Int. Ed.* **2017**, *56*, 3270; (r) A. Konishi, Y. Okada, M. Nakano, K. Sugisaki, K. Sato, T. Takui, M. Yasuda, *J. Am. Chem. Soc.* **2017**, *139*, 15284; (s) D. C. Grenz, M. Schmidt, D. Kratzert, B. Esser, *J. Org. Chem.* **2018**, *83*, 656; (t) T. Wurm, E. C. Rüdiger, J. Schulmeister, S. Koser, M. Rudolph, F. Rominger, U. H. F. Bunz, A. S. K. Hashmi, *Chem. Eur. J.* **2018**, *24*, 2735; (u) K. Sekine, F. Stuck, J. Schulmeister, T. Wurm, D. Zetschok, F. Rominger, M. Rudolph, A. S. K. Hashmi, *Chem. Eur. J.* 10.1002/chem.201803096.
- [7] (a) T. Kawase, T. Fujiwara, C. Kitamura, A. Konishi, Y. Hirano, K. Matsumoto, H. Kurata, T. Kubo, S. Shinamura, H. Mori, E. Miyazaki, K. Takimiya, *Angew. Chem. Int. Ed.* **2010**, *49*, 7728; (b) C. Liu, X. Xu, W. Zhu, X. Zhu, W. Hu, Z. Li, Z. Wang, *Chem. Eur. J.* **2015**, *21*, 17016; (c) G. Dai, J. Chang, W. Zhang, S. Bai, K.-W. Huang, J. Xu, C. Chi, *Chem. Commun.* **2015**, *51*, 503; (d) C. Li, C. Liu, Y. Li, X. Zhu, A. Wang, *Chem. Commun.* **2015**, *51*, 693.
- [8] (a) M. Nakano, I. Osaka, K. Takimiya, T. Koganezawa, *J. Mater. Chem. C* **2014**, *2*, 64; (b) M. Nakano, I. Osaka, K. Takimiya, *J. Mater. Chem. C* **2015**, *3*, 283.
- [9] (a) E. Müller, H.-G. Fritz, K. Munk, H. Straub, H. Geisel, *Tetrahedron Lett.* **1969**, *59*, 5167; (b) Z. U. Levi, T. D. Tilley, *J. Am. Chem. Soc.* **2010**, *132*, 11012; (c) J. Cao, G. London, O. Dumele, M. von Wantoch Rekowski, N. Trapp, L. Ruhlmann, C. Boudon, A. Stanger, F. Diederich, *J. Am. Chem. Soc.* **2015**, *137*, 7178.
- [10] (a) H. Clavier, S. P. Nolan, *Chem. Commun.* **2010**, *46*, 841; (b) A. Gómez-Suárez, D. J. Nelson, S. P. Nolan, *Chem. Commun.* **2017**, *53*, 2650.
- [11] CCDC 1851123 (**2a**), 1851124 (**3a**), 1851125 (**3g**), and 1851126 (**5h**) contain the supplementary crystallographic data for this paper. These data can be obtained free of charge from The Cambridge Crystallographic Data Centre via <https://www.ccdc.cam.ac.uk/structures/>
- [12] The difference of opt-electrochemical properties by the fusion pattern was described in ref. 7a and 9c. Please see the supporting information for the detail.
- [13] (a) F. Paulus, J. U. Engelhart, P. E. Hopkinson, C. Schimpf, A. Leineweber, H. Sirringhaus, Y. Vaynzof, U. H. F. Bunz, *J. Mater. Chem. C*, **2016**, *4*, 1194; (b) W. Pisula, A. Menon, M. Stepputat, I. Lieberwirth, U. Kolb, A. Tracz, H. Sirringhaus, T. Pakula, K. Müllen, *Adv. Mater.* **2005**, *17*, 684.

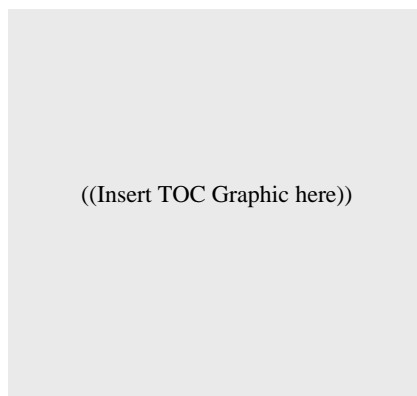
## COMMUNICATION

## Entry for the Table of Contents (Please choose one layout)

Layout 1:

## COMMUNICATION

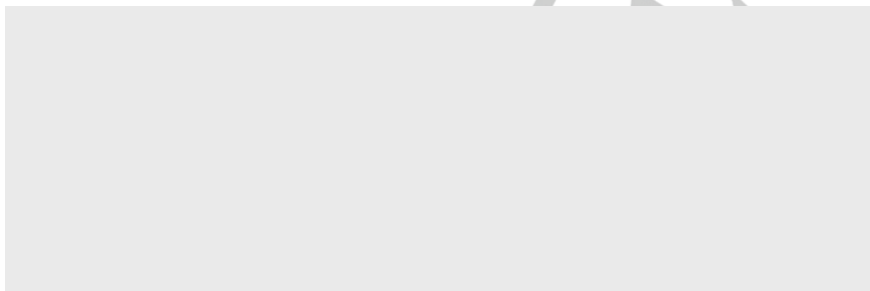
Text for Table of Contents

*Author(s), Corresponding Author(s)\****Page No. – Page No.****Title**

Layout 2:

## COMMUNICATION

The gold-catalyzed annulation of tetraynes provides a useful protocol in the synthesis of U-shaped and S-shaped bispentalenes for organic semiconductors. The naphthalene-based S-shaped naphthalene-based bispentalene shows a one dimensional face-to-face packing pattern in solid state and a good hole mobility.

*K. Sekine, J. Schulmeister, F. Paulus, K. P. Goetz, F. Rominger, M. Rudolph, J. Zaumseil,\* and A. Stephen K. Hashmi\****Page No. – Page No.****Gold-Catalyzed Facile Synthesis and Crystal Structures of Benzene-/Naphthalene-based Bispentalenes as Organic Semiconductors**